

### **DESIGN MODIFICATION IN RF INTERACTION CAVITY OF A 140GHZ GYROTRON TO ACHIEVE WIDE TUNABLE BANDWIDTH FOR DNP-NMR SPECTROSCOPY APPLICATIONS**

---

---

- 6.1. Introduction**
- 6.2. RF Interaction Cavity Design Modification**
- 6.3. Beam-Wave Interaction Exploration**
  - 6.3.1. Time-Dependent Multimode Analysis**
  - 6.3.2. PIC Simulation of the Gyrotron**
- 6.4. Conclusions**



## 6.1. Introduction

As discussed in Chapter 5, Dynamic Nuclear polarization (DNP) enhanced NMR spectroscopy desires to have a wide tunable RF source for better sensitivity required for material characterization. Keeping this as our goal, using the knowledge acquired in Chapter 5, in the current Chapter, we have revisited an experimental reported gyrotron device that operates on  $TE_{0,3}$  mode at 140GHz for 212MHz DNP-NMR applications by Joyce *et al.* 2006. It has been reported that the tunability of the RF source had been achieved by magnetic as well thermal tuning techniques. In addition, it was observed that, the gun is able to generate the maximum beam current of 25mA as well the device has been operated upto second order axial mode  $q = 2$  mode in the ideal condition. For low power tunable gyrotrons, the device can be operated in the axial mode index  $q$  from 1 to 6, that able to generate a minimum threshold power over a wide continuous frequency range without variation of  $m$  and  $p$  indices of the mode. For this, one possible way is to design longer interaction cavities thereby achieving magnetic as well electrical tuning techniques.

In this Chapter, an experimentally demonstrated low power gyrotron operating with beam voltage 12.3 kV and current 25mA at 140GHz for 212 MHz DNP NMR spectroscopy reported by Joyce *et al.* 2006 is revisited and its RF cavity design is suitably modified to enhance device tunable bandwidth by magnetic tuning. By the help of the concepts described in Chapter 5 of this thesis, for the reported RF cavity geometry with the beam parameters, the cold cavity RF characteristics and the beam wave interaction behaviour is studied as well as through PIC simulation studies are also performed using a commercial PIC code “CST Studio Suite”.

As the reported gyrotron has a limited tunable bandwidth via magnetic tuning and only thermal tuning is used. From the knowledge of the Chapter 5 about lengthy

interaction space, with the aim of achieving wider device tunable bandwidth, the tapered cylindrical RF interaction cavity is suitably modified such that in addition to thermal tuning, the magnetic tuning can also be achieved by operating the device in the high order axial operating modes using the same beam parameters. The operating mode is considered here as  $TE_{0,3,q}$  with a target of more tunable bandwidth through magnetic tuning as well. With the modified RF cavity, the cold cavity analysis and its electron-beam and RF-wave interaction behaviour studies through analysis as well as PIC simulations at various beam currents and magnetic fields are carried out.

Chapter 6, is organized as follows: for confirmation about the possible axial operating modes  $q$ , the cold cavity analysis and the start oscillation current  $I_{soc}$  curves that provide information for the state of the mode oscillation at various magnetic fields are done. Followed by the determination of RF field profiles, diffractive quality factors and resonant frequency calculations under beam absent conditions for the reported cavity and the modified cavity. The beam wave interaction mechanism in the RF cavities for various modes are studied using time dependent, non-linear, multimode theory and the same the beam wave interaction mechanisms are simulated through PIC simulation code of Commercially CST and presented. A conclusion that summarizes the current chapter is presented at the end.

## **6.2. RF Interaction Cavity Design Modification**

An RF source generates the RF energy by interacting with DC electron beam. Suitable environments are required for the successful and sustainable RF radiations with desired characteristics conditions that include selection of appropriate beam parameters, and the space that allows the interaction between electron beam and RF wave, i.e., Interaction region.

A conventional, tapered cylindrical RF interaction cavity is taken as the interaction structure in the present design. As discussed in Chapter 5, the design and optimization of an RF interaction cavity requires the knowledge of axial RF field profiles  $V_{mp}(z)$ , resonating frequencies  $f_{res}$ , and its diffractive quality factor  $Q_{diff}$  that gives the information about the amount of RF power diffracted from cavity.

For broadband tunable gyrotrons, it is advantageous to design the RF cavity which operates in the mode over a range of frequency, i.e.,  $TE_{m,p,q}$ , where the axial mode index  $q$  changes usually from 1, 2, 3 etc. This kind of implementation eases the design of the post RF interaction cavity components, i.e., nonlinear taper, collector and the RF window for the collecting and guiding the generated RF power simpler since the mode has same azimuthal and radial variations. Usually a longer interaction cavity section is chosen with  $L_c$  is of few tens of wavelengths for the smooth transitions over axial mode indices as frequency varies. Longer interaction cavities yield higher  $Q$  values. The diffractive quality factor  $Q_{diff,q}$  for the various axial mode indices are related to fundamental  $Q_{diff,1}$  as [Hornstein *et al.* (2004)]

$$Q_{diff,q} \approx \frac{Q_{diff,q=1}}{q^2} . \quad (6.1)$$

As the axial mode indices increases, the corresponding diffractive quality factor reduces by a factor of  $\sim q^2$  and it indicates about the amount of power generation is reduces too that makes the generation of stable power over tunable band of frequencies challenging. In the present work, as stated above, the RF interaction cavity designed for the 212 MHz DNP-NMR spectroscopy applications is considered; the beam and geometrical parameters are given in Tables 6.1 and 6.2. The axial RF field profiles  $V_{mp}(z)$ , resonating frequencies and corresponding diffractive quality factors  $Q_{diff}$ , under

beam absent conditions are determined by solving Vlasov approximation equations like done so far.

**Table 6.1:** Design beam parameters of Joye *et al.* (2006)

Parameter	Value
Frequency $f$	139.65 GHz
Output power $P_{out}$	> 10 W
Beam voltage $V_b$	12.3 kV
Magnetic field at the cavity $B_0$	5.06 -5.12 T
Pitch factor $\alpha$	1.6
Harmonic number, $s$	1
Beam current $I_b$	25 mA

**Table 6.2:** RF Interaction cavity dimensions of Joye *et al.* (2006)

Parameter	Value
Cavity radius $R_c$	3.48 mm
Down taper length $L_d$	5.5 mm
Down taper angle $\theta_d$	$1^\circ$
Up taper length $L_u$	36.25 mm
Up Taper angle $\theta_{up}$	$2^\circ$
Middle section Length $L_c$	28.25 mm
Resonant Frequency $f_{res}$	139.65 GHz
Diffraction quality factor $Q_{diff}$	6950

The normalized axial RF field profiles, for various possible axial modes of the reported parameters,  $q = 1, 2,$  and  $3$  with resonant frequencies along radius profile  $R(z)$

are shown in Figure 6.1. The calculated and reported resonant frequencies  $f_{res}$  as well diffractive quality factors  $Q_{diff}$  for various axial mode indices are tabulated in Table 6.3. Even though there was no mention about the existence of the axial mode index 3 but we observed the existence of it through our calculation and the corresponding details are tabulated too.

**Table 6.3:** Tailored RF cavity parameters

Mode	Reported $f_{res}$ (GHz)	Calculated $f_{res}$ (GHz)	Reported $Q_{diff}$	Calculated $Q_{diff}$
TE <sub>031</sub>	139.650	139.647	6950	6950
TE <sub>032</sub>	139.870	139.841	1750	1750
TE <sub>033</sub>	Not stated	140.241	Not stated	810

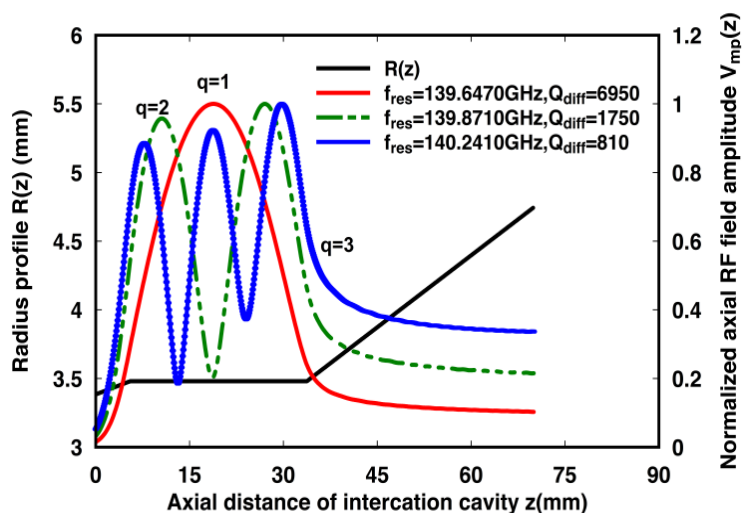


**Figure 6.1:** Normalized cold cavity axial RF field amplitude profiles for various axial mode indices TE<sub>0,3,q</sub>, where  $q = 1, 2, 3$  of Joye *et al.* (2006).

The possibility of oscillation of various modes in the cavity with respect to magnetic fields, subjected to the given beam parameters are assessed by calculating the start oscillation current curves  $I_{soc}$ . By varying the background DC magnetic field from 5 T to 5.2 T, the start oscillation current curves  $I_{soc}$  values for the operating mode TE<sub>0,3,q</sub>

at various axial indices  $q$  are calculated and are plotted in Figure. 6.2. It can be observed that the minimum current required for oscillation of the  $TE_{0,3q}$ , at  $q = 1$  and  $q = 2$ , is less than 20 mA, whereas for the  $q = 3$  mode is above 35 mA. Since, the electron gun under consideration is limited to supply the beam current of maximum 25 mA so it confirms the oscillation and growth of the high order axial modes are unattainable of mode  $TE_{0,3}$  with  $q = 3$  due to magnetic tuning and even for the excitation of  $q = 2$  mode is also challenging with given dimensions and beam parameters. Due to this limitation, the tuning of the device was achieved by varying the temperature of the coolant at the outer walls of the cavity thereby changes in the radius profile of the structure  $R(z)$  and that affects the operating frequency, i.e., via thermal tuning. It was mentioned that 0.2MHz/K is observed as per thermal cooling technique for the present design.

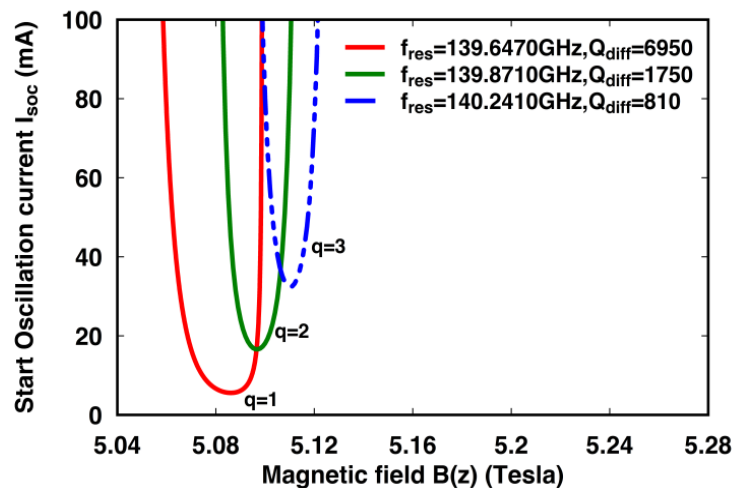


**Figure 6.2:** Start oscillation current  $I_{soc}$  (mA) versus DC magnetic field  $B$  (T) plots of  $TE_{0,3,q}$  for different axial mode indices  $q$  of Joye *et al.*(2006).

But if we are able to operate the device even in high order axial modes ( $q > 2$ ), the tunable bandwidth of the device can be improved. Targeting the enhancement of the tunable bandwidth as the priority, the dimensions of the RF interaction cavity can be modified keeping the same beam parameters, such that the device is able to operate in high order axial mode indices further. Considering the fact of longer cavities allows device to operate with low beam currents as well scope for exciting the high order axial



modes by with the surrendering the longer  $Q$  values. Since, the electron gun is limited of beam voltage 12.3 kV and beam current up to 25mA, the tailoring the cavity dimensions such that the device is able to operate for low beam currents  $I_b$  as well high axial mode operation.

The RF interaction cavity analysis using Single mode Vlasov approximation in the absence of beam is carried by considering various cavity geometrical combinations and the optimized modified dimensions are listed in Table 6.4. The corresponding RF characteristics, namely,  $f_{res}$ ,  $Q_{diff}$  of the various axial modes are tabulated in Table 6.5 and compared with the cold cavity characteristics reported by Joye *et al.* (2006).

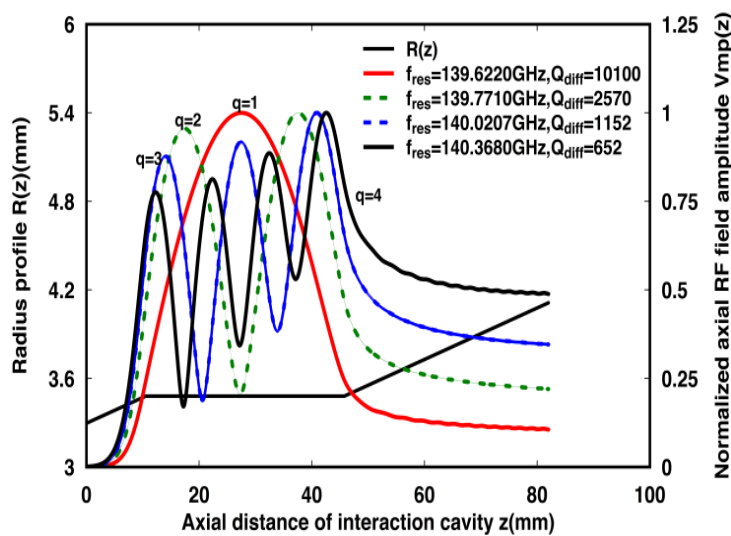
**Table 6.4:** Modified RF interaction cavity parameters

Parameters	Value
Cavity radius $R_c$	3.48 mm
Down taper length $L_d$	10.5 mm
Down taper angle $\theta_d$	$1^\circ$
Up taper length $L_u$	36.25 mm
Up taper angle $\theta_{up}$	$1^\circ$
Middle section length $L_c$	35.25 mm
Resonant frequency $f_{res}$	139.62 GHz
Magnetic field $B$	5.05 -5.20 T

**Table 6.5:** Resonating frequency  $f_{res}$  and diffractive quality factor  $Q_{diff}$  of modified cavity

Mode	Reported $f_{res}$ (GHz)	Calculated $Q_{diff}$
TE <sub>031</sub>	139.62	10100
TE <sub>032</sub>	139.771	2570
TE <sub>033</sub>	140.0207	1152
TE <sub>034</sub>	140.368	652

The cold cavity axial RF field profiles  $V_{mp}(z)$  along with radius profile  $R(z)$  of the modified cavity geometry are shown in Figure 6.3. Assigning the same beam parameters, for the modified interaction cavity, the start oscillation current curves  $I_{soc}$  are calculated over a range of magnetic fields B and are plotted in Figure. 6.4. It can be observed from the analysis that the minimum current required for the oscillation of the axial mode indices for  $q = 1, 2$  and  $3$  is less than 20mA whereas for the axial mode  $q = 4$ , it is at the verge of 25mA.

**Figure 6.3:** Normalized cold cavity axial RF field amplitude profiles of modified cavities for various axial mode indices TE<sub>0,3,q</sub>, for  $q = 1, 2, 3$ , and  $4$ .

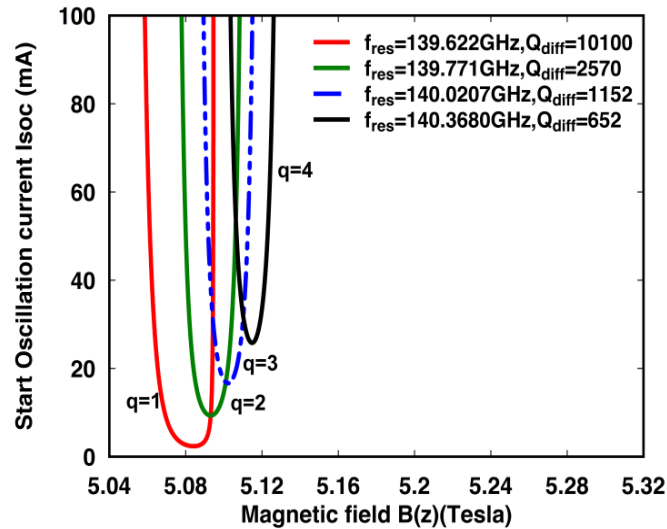


**Figure 6.4:** Start oscillation current  $I_{soc}$  (A) versus DC magnetic field  $B$  in (T) plots for different axial operating modes of  $TE_{0,3,q}$  for modified RF cavity dimensions.

From the curves, it can be observed that the minimum values of  $I_{soc}$  are reduced as compared with those reported by Joye *et al.*(2006), as well the excitation of axial mode index up to  $q = 3$  is achievable since the minimum current required is well less than 25 mA. The longer interaction cavities allow more interaction space thereby chances of more electron beam and RF wave interaction results higher output power with proper tailoring of the cavity dimensions. These are examined by studying the beam wave interaction behaviour that gives information about the temporal growth of the RF power using time dependent multimode theory as well obtained through 3D PIC simulation codes. A commercially available code “CST studio suite” is reconfigured and used for this purpose. The details of the electron beam-wave interaction studies for both the interaction cavities are carried and presented in in the following section. Though, the uptaper angle is less than the reported cavity, but the generated RF power from the RF cavity is transmitted by choosing a suitable NLT section, QOMC sections and is kept out of the scope of the present research work.

### 6.3. Beam-Wave Interaction Exploration

As discussed in the previous chapters about the beam wave interaction importance and the procedure to calculate it, using the same theory and way the beam wave interaction analysis and PIC simulations are carried out for both the reported and the modified cavity dimensions with the same beam parameters. The main details of our finding are discussed as follows.

#### 6.3.1. Time-dependent multimode analysis

In the present study, selecting a uniform background DC magnetic field profile  $B(z)$  along the interaction length, the coupled equations are numerically integrated using fourth order Runge-Kutta method. A 12.3 kV DC voltage is applied to a uniformly distributed gyrating electron beam carrying a current of 25mA having 16 beamlets with 16 electrons in each beamlets. For the operating and its neighbouring modes, like,  $TE_{2,3}$ ,  $TE_{0,2}$ , the beam-wave interaction calculations are done. Taking various magnetic field values, the temporal growth of RF powers in the output mode for both the designs with respect to the time has been determined. The temporal growth of RF power in the main mode  $TE_{0,3,1}$  for both the cavities are determined analytically and plotted in Figure.6.5. The RF powers of the operating modes for various magnetic fields are calculated while providing the various axial mode index profiles with the corresponding frequencies for both the designs and are plotted in Figure. 6.5. For both cavities designs, the analytical calculations are carried out by taking the beam current 25mA.

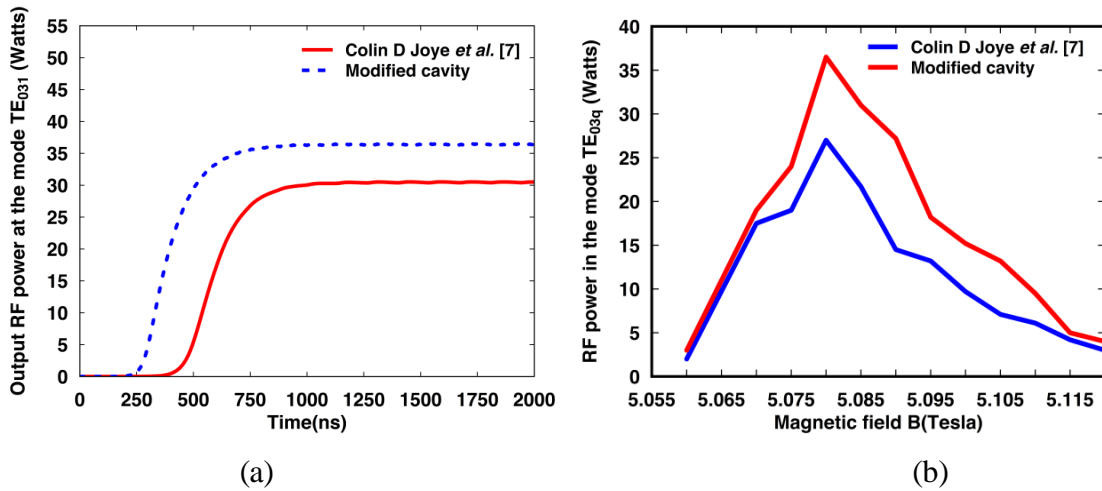


**Figure 6.5:** Comparisons of RF power (a) versus time using multimode analysis and (b) with respect to magnetic fields for cavities of Joye et al. (2006) and modified design.

### 6.3.2. PIC simulation of the gyrotron

In addition to the non-linear multimode analysis, like in the Chapter 3 and 4, using 3D particle in cell solver, simulation of the electron beam and RF-wave interaction mechanisms of the device is performed reconfiguring a commercial code “CST Studio Suite” for both the cavity geometries. In the present study, the modelled is designed in CST studio suite selecting OFHC copper as the cavity material with conductivity of  $2.9 \times 10^7$  S/m by assigning suitable boundary conditions. A DC particle source is taken for forming the gyrating electron beam with assigned parameters, and a uniform magnetic field profile is applied along the device structure axis.

For observing the time varying behaviour of modes, various 3D E-field and H-field monitors are placed with suitable boundary conditions. The PIC simulation has run for 1000 ns and after the simulation time, by performing post processing steps, the necessary information for confirmation of the device design has been carried out.

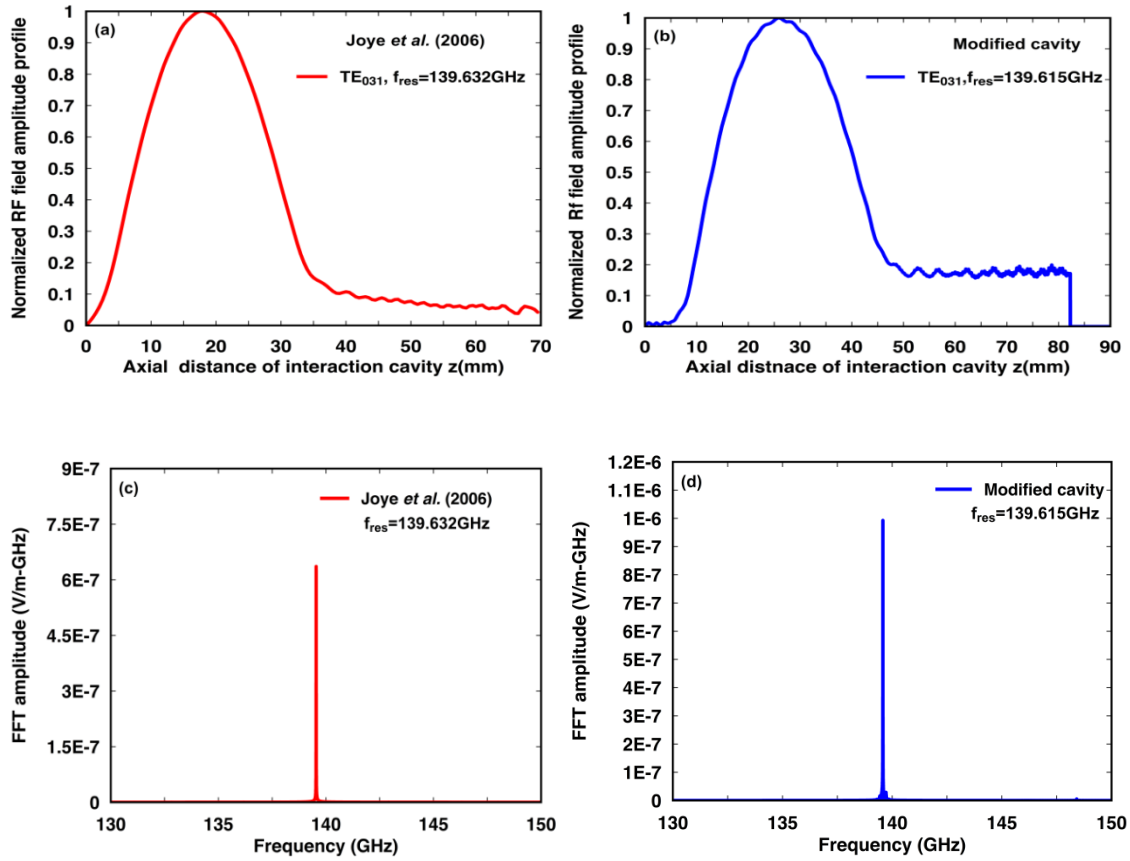


**Figure 6.6:** PIC Simulation results - (a-b) hot axial RF field profiles (c-d) frequency response of the operating mode  $TE_{0,3,q}$  with axial index  $q = 1$  for cavities of Joye et al.(2006) and modified designs, respectively.

The PIC simulated results for both the designs at beam current  $I_b = 25$  mA and magnetic field 5.08 T are shown in Figures 6.9 and 6.7. The axial RF field profile in the presence of the electron beam along with the fast Fourier transform of the mode is shown in Figure 6.6. The temporal growth of mode amplitudes and the peak power generated in the mode  $TE_{0,3,1}$  mode is shown in Figure 6.7.

It is found that the operating mode oscillates at 139.63 GHz for the reported cavity dimensions and able to generate power of  $\sim 23$ W whereas for the modified cavity it has been observed that a stable RF power of more than  $\sim 27$ W oscillating at 139.59 GHz in the fundamental axial mode of  $TE_{031}$  for a beam current of 25 mA at magnetic

field 5.08 T. The results are shown for the external magnetic field of a 5.08 T uniform magnetic field along the interaction structure.

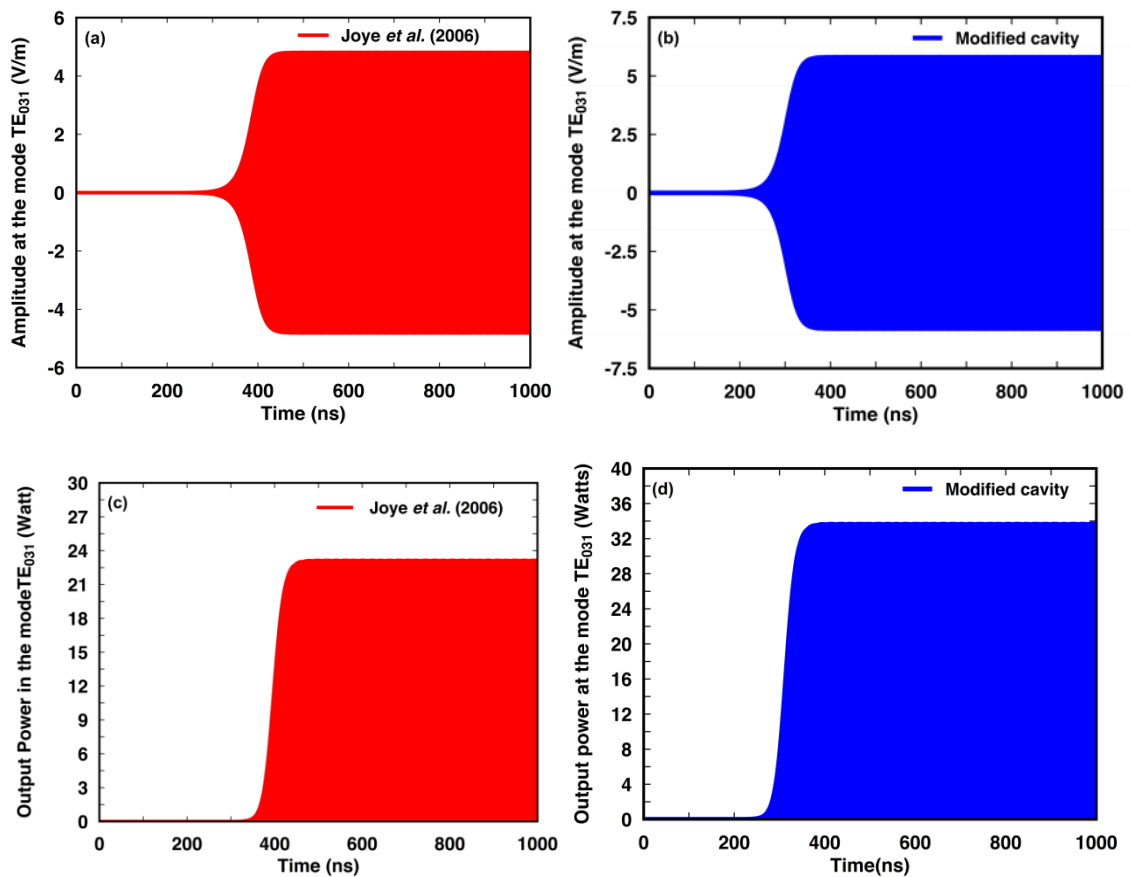


**Figure 6.7:** PIC Simulation results - Temporal growth of mode TE<sub>0,3,1</sub> (a - b) amplitudes (c - d) power values for cavities reported design by Joye *et al.* (2006) and as per our modified design, respectively.

Even an amount of more than 15W power is observed in the second axial mode index of TE<sub>0,3,2</sub> oscillating at 139.76 GHz for beam current of 25 mA at magnetic field of 5.11 T. By operating the device in the high order axial modes, through magnetic tuning, the operating bandwidth found to be enhanced.

## 6.4. Conclusions

A low power, tunable gyrotron operating in a TE<sub>0,3,q</sub> mode for 140 GHz DNP NMR spectroscopy applications is explored to facilitate wider bandwidth with magnetic tuning. The RF interaction cavity design has been tailored such that it can operate in the

high order axial modes. The beam absent as well as beam present RF wave behaviour, both analytical and Particle-in-Cell (PIC) simulation studies have been presented. Gyrotron beam-wave interaction behaviour explored using time dependent non-linear multi-mode analysis for various beam currents and magnetic fields and more than >15W of RF power over a tunable bandwidth of 400MHz has been achieved through magnetic field tuning for the tailored the interaction cavity. More than 15W RF power output over a band of 400 MHz through magnetic tuning has been attained solely apart from thermal tuning at beam currents of around 25 mA. The thermal tuning behaviour for the modified cavity is kept beyond the scope of the present research. In addition, a 3D PIC simulation for fundamental modes  $TE_{031}$ , at beam currents 25mA for both the designs have been carried out and it was found that the modified design gives more power compared with reported design due to lengthy interaction space. Further, it was also observed that, the time required for the growth of RF power gets reduced for the modified cavity. This tunable bandwidth gyrotron design provides important application for the enhancement of sensitivity of the DNP NMR spectroscopy.

Though, the cavity has been tailored for enhancement of bandwidth, but the suitable after cavity components are also need to be designed such that the generated RF quantity and is to carried to the output transmission system. Due to the tunability nature of the RF quantity, the design of nonlinear taper, Quasi-optical mode converter as well RF window becomes little bit complex and these are not kept within the scope of the present research work.